# TWO-DIMENSIONAL WAVE SPECTRA IN THE TROPICAL WESTERN PACIFIC OCEAN DURING THE MONEX CRUISE

Mizuno, Shinjiro
Research Institute for Applied Mechanics, Kyushu University : Associate Professor

Honda, Tadao
Research Institute for Applied Mechanics, Kyushu University : Research Assistant

Mitsuyasu, Hisashi
Research Institute for Applied Mechanics, Kyushu University : Professor

https://doi.org/10.5109/6777128

出版情報：Reports of Research Institute for Applied Mechanics. 29 (91), pp.95-104, 1981-07. 九州大学応用力学研究所
バージョン：

Reports of Research Institute for Applied Mechanics
Vol. XXIX, No. 91, 1981

# TWO-DIMENSIONAL WAVE SPECTRA IN THE TROPICAL WESTERN PACIFIC OCEAN DURING THE MONEX CRUISE

By Shinjiro MIZUNO*, Tadao HONDA** and Hisashi MITSUYASU***

During the MONEX cruise ocean waves were measured at a fixed station (2°N, 140°E) and at a trade wind ocean area (10°N, 150°E) using a cloverleaf buoy, and wave data of 20 runs of 45 min duration were obtained under relatively low wind conditions.

Using these data it is shown that the principal direction of waves relative to the buoy orientation has an important effect on the maximum value of the spreading parameter $S_{2,max}$, which is a measure of the concentration of the directional distribution of waves at the spectral distribution.

***Key words***: MONEX, Cloverleaf buoy, Two-dimensional wave spectra

## 1. Introduction

In recent studies on two-dimensional spectrum of ocean waves several standard forms of the angular distribution function about the mean wave direction have been proposed by some authors such as Mitsuyasu *et al.*[1] and Hasselmann *et al.*[2]. In these studies the scatter of the data around the proposed relation is still much larger than might be expected, as pointed out by Hasselmann *et al.*

Therefore, it seems to be important to investigate some possible causes of the scatter at the present time.

In this report we present some characteristics of the power spectrum and the directional spectrum of ocean waves observed at the Western Pacific ocean during the Monsoon Experiment (MONEX) cruise and con-

* Associate Professor, Research Institute for Applied Mechanics, Kyushu University.

** Research Assistant, Research Institute for Applied Mechanics, Kyushu University.

*** Professor, Research Institute for Applied Mechanics, Kyushu University.

sider a possible cause of the scatter of the data measured during the cruise. It will be shown that the principal direction of the waves relative to the buoy orientation has a considerable influence on the maximum value of the spreading parameter $S_{max}$, of the angular distribution function.

## 2. Wave observations

During the MONEX cruise (1 May-9 June, 1979), waves were measured at two areas of the Western Pacific ocean using a cloverleaf buoy. The research vessel Hakuhō-Maru stayed at the fixed station (2°N, 140°E) for about 2 weeks and many different types of meteorological and oceanographic observations were made to investigate the physical processes associated with monsoons[3]. The wave data were recorded continuosly on analog cassette tape for 6h a day on the first 2 and last 2 days of the drifting state. On our return cruise from Rabaul to Tokyo along the longitude 150°E we came across a typical trade wind of 8–9 m/s at 10°N, measuring the waves for about one hour there. Altogether, 20 runs of 45 min duration were obtained during the cruise. The date, time and locations of wave observations are summarized in Table 1 together with

Table 1. H: significant wave height ($H=2.83\sqrt{2E}$, $E=\int_{f_c}\phi(f)\,df$, $f_c=0.05$ Hz), T: wave period, $\theta_s$: swell direction, $\theta_w$: wind-wave direction, $\theta_u$: wind direction, U: wind speed.

Wind and wave data (1979)

| Run | Date | Time | Locations | H (m) | T (sec) | $\theta_s$ | $\theta_w$ | U (m/sec) | $\theta_u$ |
|---|---|---|---|---|---|---|---|---|---|
| 1 | May 4 | 13 : 26–13 : 50 | 22°00.5N–139°59.7E | 1.7 | 8.2 | E | | 5.0 | E |
| 2 | May 10 | 10 : 00–10 : 45 | 2°00.8N–140°00.6E | 1.5 | 10.8 | E | | 2.0 | SE |
| 3 | 10 | 11 : 00–11 : 45 | 2°01.2N–140°00.7E | 1.7 | 10.4 | E | | 2.0 | E |
| 4 | 10 | 12 : 00–12 : 45 | 2°01.5N–140°00.5E | 1.6 | 10.8 | E | | 2.5 | NE |
| 5 | 10 | 13 : 00–13 : 45 | 2°01.7N–140°00.2E | 1.7 | 10.6 | ENE | | 3.5 | ENE |
| 6 | 10 | 14 : 00–14 : 45 | 2°02.0N–139°59.8E | 1.6 | 10.9 | E | | 3.0 | ENE |
| 7 | 10 | 15 : 00–15 : 45 | 2°02.1N–139°59.2E | 1.7 | 10.5 | E | | 3.0 | ENE |
| 8 | May 20 | 9 : 45–10 : 30 | 1°57.9N–140°00.7E | 1.4 | 7.3 | NNE | NNW | 6.0 | NNW |
| 9 | 20 | 10 : 50–11 : 35 | 1°56.5N–140°00.6E | 1.2 | 9.2 | N | NNW | 6.0 | NNW |
| 10 | 20 | 11 : 45–12 : 30 | 1°55.1N–140°00.4E | 1.3 | 7.6 | NNE | NNW | 5.5 | NNW |
| 11 | 20 | 12 : 45–13 : 30 | 1°53.5N–140°00.3E | 1.3 | 7.5 | NNE | NNW | 6.0 | NNW |
| 12 | 20 | 13 : 45–14 : 30 | 1°52.0N–140°00.3E | 1.3 | 7.5 | NNE | NNW | 6.0 | NNW |
| 13 | 20 | 14 : 45–15 : 30 | 1°50.4N–140°00.3E | 1.2 | 8.1 | NNE | NNW | 6.0 | NNW |
| 14 | May 21 | 9 : 25–10 : 10 | 1°57.2N–139°59.8E | 1.2 | 7.7 | NNE | NW | 5.0 | NW |
| 15 | 21 | 10 : 25–11 : 10 | 1°56.0N–139°59.6E | 1.2 | 8.6 | NNE | NW | 5.0 | WNW |
| 16 | 21 | 11 : 25–12 : 10 | 1°54.5N–139°59.5E | 1.2 | 8.4 | NNE | NNW | 4.5 | NW |
| 17 | 21 | 12 : 25–13 : 10 | 1°53.2N–139°59.5E | 1.1 | 9.5 | NNE | NW | 5.0 | NW |
| 18 | 21 | 13 : 25–14 : 10 | 1°51.8N–139°59.7E | 1.2 | 9.3 | NE | NW | 5.0 | NW |
| 19 | 21 | 14 : 25–15 : 10 | 1°50.5N–140°00.0E | 1.1 | 9.2 | NE | NW | 5.5 | WNW |
| 20 | June 2 | 13 : 05–13 : 50 | 10°30.1N–150°08.9E | 1.4 | 6.7 | | E | 7.0 | E |

wind and wave data.

### 3. Data analysis

Only three of six signals of the cloverleaf buoy, i. e., the vertical acceleration $s_1=\eta_{tt}$ and the two components of the wave slope $s_2=\eta_x$ and $s_3=\eta_y$, were used for the analysis. Cross spectra $C_{lm}(f)-iQ_{lm}(f)$ were calculated using FFT procedure, where $l, m=1, 2, 3$. The subsequent spectral analysis is almost the same as that described by Mitsuyasu *et al.*[1]:

| | |
|---|---|
| Sampling interval: | $\Delta t = 0.4$ s |
| Data points for one segment: | $N = 2048$ |
| Sample length for one segment: | $T_N \doteqdot 13.6$ min |
| Nyquist frequency: | $f_N = 1.25$ Hz |
| Elementary frequency bandwidth: | $\Delta f_0 = 1.22\times10^{-3}$Hz |
| Spectral filter: | $\overline{\Delta f} = 2.44\times10^{-2}$Hz |
| Equivalent dagrees of freedom: | $df = 126$ |

Usually each run of 45 min duration was divided into 3 non-overlapping segments of equal length and the final cross spectra were obtained by averaging over them, execept for the runs, for which the buoy changed its orientation considerably during the measurements.

Now the method of analysis follows those originally proposed by Longuet-Higgins *et al.*[3] and by Cartwright and Smith[4]. The directional spectrum $E(f, \theta)$ is expressed in the form,

$$E(f,\theta)=\phi(f)\cdot h(f,\theta)\ , \tag{1}$$

where $\phi(f)$ is the one-dimensional wave spectrum and $h(f, \theta)$ the normalized angular distribution function. $\phi(f)$ is obtained from the acceleration spectrum $C_{11}(f)$, i. e.,

$$\phi(f)=(2\pi f)^{-4}C_{11}(f)\ . \tag{2}$$

Using the dispersion relation of waves we obtain the following relation

$$C_{11}(f)=C_{22}(f)+C_{33}(f)\ , \tag{3}$$

where $C_{22}(f)$ and $C_{33}(f)$ are the pitch and roll spectra, respectively. If $h(f, \theta)$ is expanded into the Fourier series

$$h(f,\theta)=\frac{1}{\pi}\left\{\frac{1}{2}+\sum_{n=1}^{\infty}a_n\cos u\theta+\sum_{n=1}^{\infty}b_n\sin n\theta\right\} \tag{4-a}$$

$$=\frac{1}{\pi}\left\{\frac{1}{2}+\sum_{n=1}^{\infty}C_n\cos n(\theta-\theta_n)\right\}\ , \tag{4-b}$$

then the Fourier coufficients up to the second terms are related to the cross spectra ($C_{lm}$, $Q_{lm}$) as follows:

$$a_1=\frac{Q_{12}}{C_{11}}, \quad b_1=\frac{Q_{13}}{C_{11}}, \tag{5-a}$$

$$a_2=\frac{C_{22}-C_{33}}{C_{22}+C_{33}}, \quad b_2=\frac{2C_{23}}{C_{22}+C_{33}}, \tag{5-b}$$

and

$$C_1=\sqrt{a_1^2+b_1^2}, \quad C_2=\sqrt{a_2^2+b_2^2} \tag{5-c}$$

On the other hand, the measured angular distribution function is usually fitted to the unimodal form

$$h(f,\theta)=G\left|\cos\frac{1}{2}(\theta-\theta_n)\right|^{2S_n} \tag{6}$$

where G is a normalizing constant. Among a series of $S_n$ and $\theta_n$, the spreading parameters $S_1$ and $S_2$ and the mean wave directions $\theta_1$ and $\theta_2$ are most concerned with the present study and related to the Fourier coefficients

$$C_1=\frac{S_1}{S_1+1}, \quad C_2=\frac{S_2(S_2-1)}{(S_2+1)(S_2+2)} \tag{7-a, b}$$

and

$$\theta_1=\tan^{-1}\frac{b_1}{a_1}=\tan^{-1}\frac{Q_{13}}{Q_{12}}, \quad 2\theta_2=\tan^{-1}\frac{b_2}{a_2}=\tan^{-1}\frac{2C_{23}}{C_{22}-C_{33}}. \tag{8}$$

## 4. Results and discussions

In the beginning let us compare the power spectrum of the acceleration $C_{11}$ with that of the slope $C_{22}+C_{33}$. Fig. 1 (a), in which all the buoy signals were in normal operation, shows that the relation of Eq. (3) is rather well satisfied between 0.05 Hz and 0.5 Hz, although considerable differences in the values of both the spectra are apparent below 0.05 Hz and above 0.5 Hz. Since the signals below 0.05 Hz are in noise level, they are cut off in the actual spectral computation. Also the effects of finite dimension of the buoy could not be neglected above 0.5 Hz, or for the waves of wave length shorter than 6 m. Therefore the effective frequency range of the buoy is available between 0.05 and 0.5 Hz. In case of Fig. 1 (b) the accelration signal was contaminated by a large number of intermittently generating random noises. Note, then that $C_{11}$ is nearly white spectrum.

The one-dimensional wave spectrum $\phi(f)$, the mean wave direction $\theta_1$ and the spreading parameters $S_1$ and $S_2$ are shown as a function of the wave frequency f in Figs. 2-5. Before the voyage we expected that we might measure swell waves of big power at the tropical ocean.

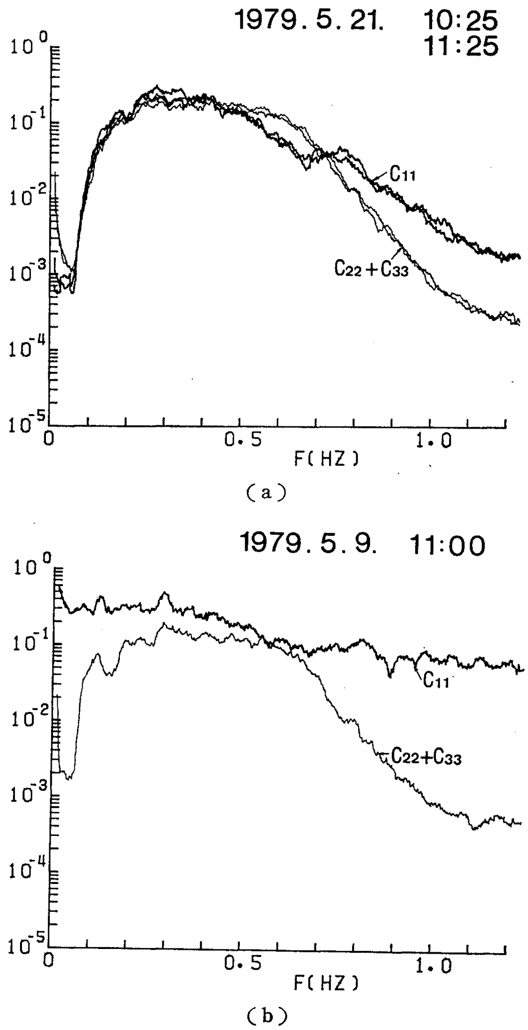


Fig. 1. Comparison of $C_{11}(f)$ and $C_{22}(f)+C_{33}(f)$ for typical wave data. (a) in case of normal operation, (b) the acceleration signal is abnormal.

As shown in Table 1 and Figs. 2–4, however, we had no good chance of measuring significant swell waves there, because tropical cyclones did not generate near the fixed station during the stay. On our return cruise we came across a typical trade wind of 8–9 m/s at 10°N. Before measuring the waves the local wind continued to blow more than 8h from the east and the wind waves were developing rapidly. The one-dimen-

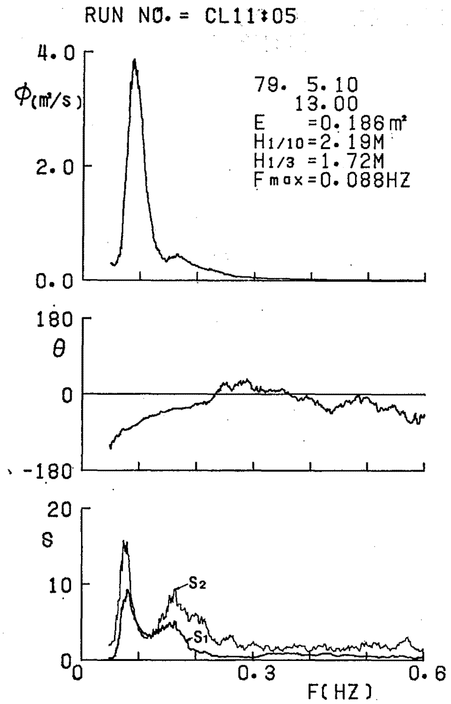


Fig. 2. Typical example of one-dimensional wave spectrum $\phi(f)$, the mean wave direction $\theta_1(f)$, and the spreading parameters $S_1(f)$ and $S_2(f)$ obtained during the MONEX cruise.

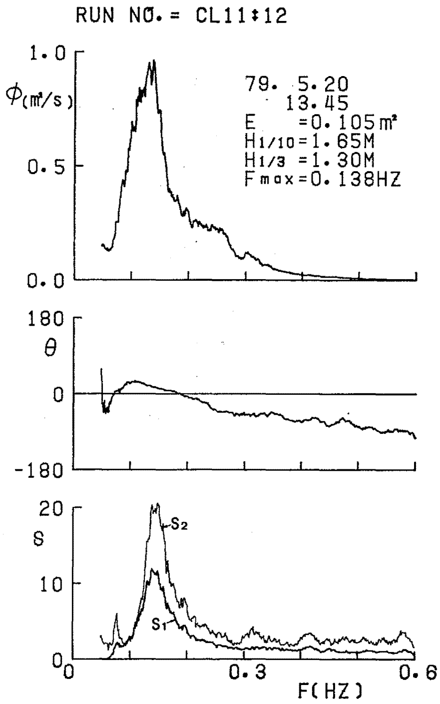


Fig. 3. For legend see Fig. 2.

sional wave spectrum $\phi(f)$ for this run is shown in Fig. 5, which has two peaks possibly due to the swell and local wind waves, although we did not visually observe the swell waves.

Now Mitsuyasu *et al.* proposed a standard form of the angular distribution function of the directional spectrum, using the wave data measured by the cloverleaf buoy. According to Mitsuyasu *et al.* the spreading parameter $S(f)$ has its maximum value $S_{max}$ near the spectral peak frequency $f_m$, decreasing rapidly toward the higher and lower wave frequencies. Thus $S_{max}$ is the most important parameter that characterizes the concentration of the directional distribution of a wave system.

For the local wind-generated waves $S_{max}$ is empirically given by them

$$S_{max} = 11.5\left(\frac{2\pi f_m U}{g}\right)^{-2.5}, \tag{9}$$

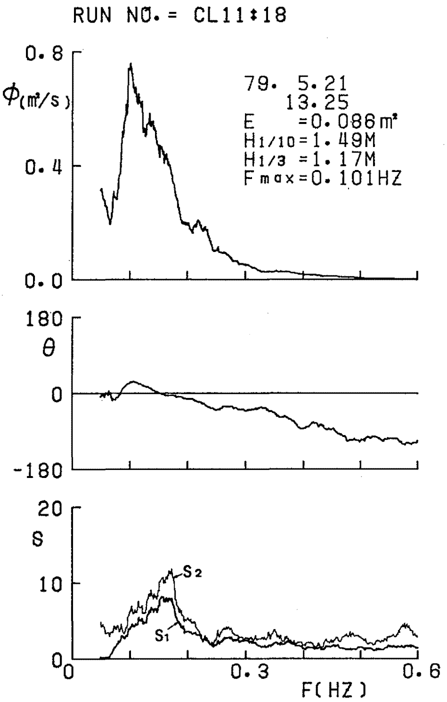


Fig. 4. For legend see Fig. 2.

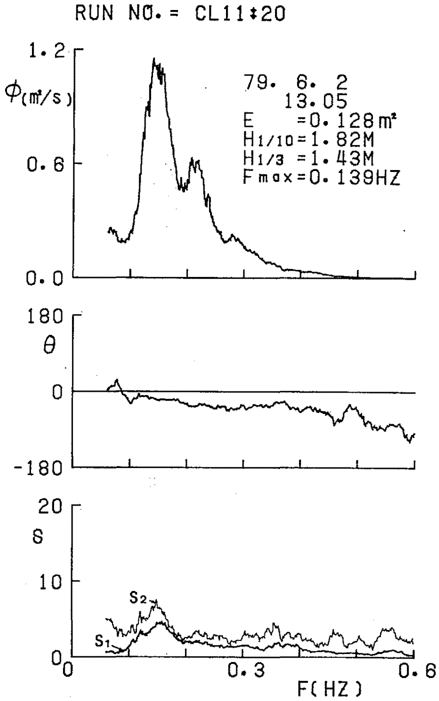


Fig. 5. For legend see Fig. 2.

where U is the the wind speed and g the acceleration of gravity.

By applying eq. (9) to the present data (Run. 20), we obtain $S_{max} \approx 26$. On the other hand, we find that $S_1$ and $S_2$ for the same run (Fig. 5) are an order of magnitude less than $S_{max}$ obtained from eq. (9). This is why? One reason might be given by Long[5], who insisted that the statistical validity of a model spectrum must be checked. By doing so, Long (1980) showed that the unimodal fitting procedure(Eq. (6)) is inadequate for estimating the directional properties of the one-dimensional wave spectrum which has two spectral peaks; caused by swell and a local wind wave. Thus, the estimates of $S_1$ and $S_2$ for Run. 20 are statistically invalid, because the one-dimensional wave spectrum has two peaks. As described just before, however, we did not visually observe significant swell waves at the trade wind area, so that the reduction of $S_{max}$ might be due to another reason.

Though it is in itself a measure of the directional spreading of the waves, the spreading parameter $S(f)$ also depends on the frequency response of the buoy, which is also a function of the wave direction relative to the buoy orientation as well as the wave frequency. It is therefore of interest to investigate to what extent the maximum value

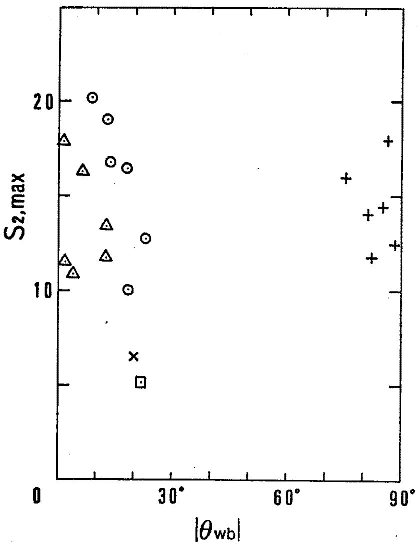


Fig. 6. $S_{2,\max}$ is plotted against $\theta_{wb}$, which is the angle between the principal direction of the waves and the buoy orientation. ⊡: the data for 4 May, +: those for 10 May, ⊙: those for 20 May, ⚠: those for 21 May, ×: those for 2 June.

of the spreading parameter $S_{\max}$ depends on the wave direction relative to the buoy orientation. For all the runs presented in Table 1, $S_{2,\max}$ were plotted against $\theta_{wb}$ in Fig. 6, where $S_{2,\max}$ is the maximum value of $S_2(f)$ and $\theta_{wb}$ the angle between the mean wave direction and the buoy orientation at the wave frequency corresponding to $S_{2,\max}$. The data of the same date plotted in Fig. 6, especially those of 20 May (circles) and 21 May (triangles) are worth noting. The wind and wave conditions were kept nearly unchanged during the two days; that is, light wind of 5-6 m/s continued to blow from NNW throughout the period, swell as well as local wind-waves observed visually to come from the same direction as the wind, though $\theta_{wb}$ gradually changed while the R. V. was drifting. It is also clear from Table 1 that the swell waves were gradually decaying during the period. Nevertheless, Fig. 6 shows that $S_{2,\max}$ depends strongly on $\theta_{wb}$ when we take notice of the same symbols only, and that they are somewhat higher for a group of the circles than for that of the triangles. When we recall the fact that the swell was gradually decaying, this suggests that the waves tend to spread while decaying. Fig. 6 also shows that $S_{2,\max}$ tends to decrease with increasing $\theta_{wb}$ for $\theta_{wb} < 30°$. Note that $\theta_{wb}$ has a rather large value for Run 20 (cross). This is perphaps one of the reasons why $S(f)$ is low for Run 20.

Finally we briefly discuss why $S_{2,\max}$ depends on $\theta_{wb}$. When $\theta_{wb}$ is close to zero, $C_{23} \doteqdot 0$. Then Eqs. 5 (b) and (c) reduce to

$$C_2 \doteqdot \frac{C_{22}-C_{33}}{C_{22}+C_{33}} \equiv a_2 \ . \tag{10-a}$$

In this case we obtain from Eq. 7 (b) the following approximate relation

$$S_{2,\max} \doteqdot 2\frac{C_{22}}{C_{33}} -1 \ . \tag{11}$$

This relation suggests that $S_{2,\max}$ could take very high values for $\theta_{wb}$ near zero, for then it is possible that $C_{22} \gg C_{33}$. On the other hand, when $\theta_{wb}$ is close to 45°, $C_{22} \doteqdot C_{33}$. Then, Eqs. 5 (b) and (c) reduce to

$$C_2 \doteqdot \frac{2C_{23}}{C_{22}+C_{33}} \equiv b_2 \ . \tag{10-b}$$

In this case $C_2$ or $S_2$ is primarily determined by the co-spectrum $C_{23}$, which is usually low as compared to the sum of $C_{22}$ and $C_{33}$, partly because the coherence between $\eta_x$ and $\eta_y$ is not good over the whole frequency, and partly because the phase difference between $\eta_x$ and $\eta_y$ produced possibly by the phase shift of the buoy signals reduces $C_{23}$. Thus, $S_{2,\max}$ tends to become smaller and smaller as $\theta_{wb}$ in creases from zero to 45°.

In conclusion, the MONEX data have shown that $S_{2,\max}$, depends not only on the concentration of the directional spectrum but also on $\theta_{wb}$, the angle between the mean wave direction and the buoy orientation.

## Acknowledgements

The present study is part of the summer field experiment of the MONEX cruise or the KH-79-2 cruise of the R. V. Hakuho-Maru. The authors would like to thank Professor T. Asai, Chief scientist aboard for his sincere arrangements, and Captain I. Tadama and all the crews of the R. V..

The spectral calculation was made using the MELCOM-900 computer system of Research Institute for Applied Mechanics. The authors are also deeply indebted to Mr. M. Ishibashi for computer analysis of wave data, to Mr. K. Marubayashi for buoy maintenance, and to Miss M. Hojo for typing the manuscript.

## References


1) Mitsuyasu, H., Tasai, F., Suhara, T., Mizuno, S., Ohkusu, M., Honda, T., and Rikiishi, K.: Observations of the directional spectrum of ocean waves using a cloverleaf buoy, J. Phys. Oceanogr. **5** (1975) 750.
2) Hasselmann, D. E., Dunckel, M. and Ewing, J. A.: Directional wave spectra observed during JONSWAP 1973, J. Phys. Oceanogr. **10** (1980) 1264.
3) Ed. by Asai, T. : Preliminary report of the Hakuho-Maru cruise KH-79-2 (MONEX cruise), Ocean Research Institute, University of Tokyo, (1979).
4) Longuet-Higgins, M. S., Cartwrighi, D. E. and Smith, N. D.: Observations of the directional spectrum of sea waves using the motions of a floating buoy. Ocean Wave Specfra, Prentice Hall, (1963) 111.
5) Cartwright, D. E.: The use of directional spectra in studying the output of the wave-recorder on a moving ship. Ocean Wave Spectra, Prentice Hall, (1963) 203
6) Long, R. B.: The statistical evaluation of directional spectrum estimates derived rom pitch/roll buoy data, J. Phys. Oceanogr. **10** (1980) 944.


(Received May 1, 1981)